Critical dynamics of randomly assembled and diluted threshold networks

Karl E. Kürten[1,2] and John W. Clark[3,4]
[1]*Fakultät für Physik, Universität Wien, Austria*
[2]*Department of Physics, Loughborough University, LE11 3TU, United Kingdom*
[3]*McDonnell Center for the Space Sciences and Department of Physics, Washington University, St. Louis, Missouri 63130, USA*
[4]*Institut für Theoretische Physik, Johannes Kepler Universität, A-4040 Linz, Austria*
(Received 3 August 2007; revised manuscript received 11 January 2008; published 24 April 2008)

The dynamical behavior of a class of randomly assembled networks of binary threshold units subject to random deletion of connections is studied based on the annealed approximation suitable in the thermodynamic limit. The dynamical phase diagram is constructed for several forms of the probability density distribution of nonvanishing connection strengths. The family of power-law distribution functions $\rho_0(x)=(1-\alpha)/(2|x|^{\alpha})$ is found to play a special role in expanding the domain of stable, ordered dynamics at the expense of the disordered, "chaotic" phase. Relationships with other recent studies of the dynamics of complex networks allowing for variable in-degree of the units are explored. The relevance of the pruning of network connections to neural modeling and developmental neurobiology is discussed.

DOI: 10.1103/PhysRevE.77.046116 PACS number(s): 89.75.−k, 87.18.Sn, 68.35.Rh, 05.45.−a

I. INTRODUCTION

Theoretical and intuitive understanding of the topological properties and dynamical behavior of complex networks has assumed increasing importance over the last several decades, with the growing recognition of the ubiquitous role of these systems in the natural and social sciences. Among other milestones, one can point to the neural-network models introduced and analyzed by McCulloch and Pitts [1], Caianiello [2], and Hopfield [3], to Kauffman's seminal Boolean model of gene-regulation networks [4,5], to the small-world networks of Watts and Strogatz [6], and to the scale-free networks studied by Barabáshi and Albert [7,8].

The present contribution extends the analysis of the dynamics of randomly assembled and diluted threshold networks begun in the 1980s [9–13]. This early work established the existence of two dynamical phases, ordered (or "frozen") and disordered (or "chaotic"), and implemented a prescription for determining the critical boundary between the phases. In the frozen phase, a dynamical system that can be adequately modeled by such a network would exhibit stable operation, robust against disturbance, but it would be subject to damage spreading and failure in the chaotic phase. (Alternatively, the chaotic phase may have an important role in giving access to more flexible behavior.) Interest in this criticality problem has revived in recent years, for both random threshold network models [22,23] and random Boolean nets [24]. Our specific aim in the present work is to explore the extent to which the stable regime can be expanded by adjusting the choice of probability density distribution for the strengths of connections in a diluted random threshold network. Among the choices examined, the power-law (or "scale-free") distribution is found to have particularly interesting properties.

In Sec. II, a general class of randomly assembled networks of binary processing units is defined in terms of the topology of connections among the units and a dynamical update rule. Section III continues with statistical specification of the network models to be studied in terms of probability distributions for the number of connections to a given unit and for the strengths of those connections. Known results [11] for the two-phase dynamical behavior of such models as determined within the annealed approximation [14–17] are reviewed for the case that all units receive the same number of connections. The critical analysis is extended to allow for variation in the number of incoming connections to the processing units. Statistical specification of the network models is completed in Secs. IV and V, with the introduction of an algorithm for random deletion of connections (dilution of the network) and with the selection of four different probability density distributions governing the strengths of surviving connections. For each of the selected distributions, results are obtained for the critical mean connectivity, which defines the boundary between the chaotic and frozen dynamical domains and hence decides the relative stability of the competing models. Section VI is devoted to an interpretation of these results (which favor the power-law distribution), to a comparison of our findings with those of somewhat related theoretical studies, and to a brief discussion the roles of synapse elimination (dilution of network connections) in neurobiology and neural modeling.

II. RANDOMLY CONNECTED THRESHOLD MODELS

The models to be studied here belong to the class of randomly assembled threshold networks [18,19]. A given network is made up of N interacting units i that occupy one of two states. In the most common examples, such units may represent Ising spins or McCulloch-Pitts "on-off" neurons. Thus, we introduce for each unit a binary state variable $\sigma_i \in \{-1,+1\}$, with values -1 and $+1$ corresponding, respectively, to spin up and spin down in the Ising case or to "firing" and "not firing" in the case of impoverished neurons. The dynamical state of the system as a whole is formed by concatenation of the individual state variables, $\sigma = \{\sigma_1 \cdots \sigma_i \cdots \sigma_N\}$. There exists a pattern of directed connections between the units, forming a network in which units stimulate one another, potentiating state changes (analogous

to "spin flips"). More specifically, an arbitrary unit i receives inputs (connections) from k_i other units of the system, with $1 \leq k_i \leq N-1$ (thus excluding self-interaction). It is convenient to introduce an $N \times N$ connection matrix (c_{ij}), such that element c_{ij} vanishes if i receives no connection from unit j and otherwise measures the strength or "weight" of the connection or coupling from j to i $(j \to i)$. The number of incoming (outgoing) connections to (from) a given unit i is commonly referred to as its *in-degree* (*out-degree*).

The time evolution of the system obeys a linear threshold rule, the states of the individual units being updated in parallel in discrete time according to

$$\sigma_i(t+1) = \mathrm{sgn}\left[\sum_j c_{ij}\sigma_j(t) + h\right]. \tag{1}$$

Thus, for specified connection strengths c_{ij} and threshold $(-)$ or bias $(+)$ parameter h, the state of unit i at the next time-step $t+1$ depends only on the binary state values of its input units at the previous time step t. (We shall assume uniform thresholds; i.e., the parameter h is taken the same for all units.) The stimuli $c_{ij}\sigma_j$ from the input units of i are superposed linearly before executing the threshold operation. In the spin example, the quantity in square brackets in Eq. (1) may be interpreted as the "local field" acting on unit i, due to interactions with the other units j and due to an external field represented by h. It should be stressed that in general the connection matrix (c_{ij}) is not symmetric. In other words, the action of unit j on unit i is generally different from the action of i on j. Moreover, the nonvanishing c_{ij} can take on positive or negative values, corresponding to the "excitatory" or "inhibitory" effect of unit j on unit i.

As described, a model of the kind we have selected for study may be viewed as a complex network (e.g., a neural network) evolving synchronously in time under a linear threshold dynamics (where "linear" refers to linear superposition of inputs prior to application of the threshold nonlinearity). Alternatively, the model may be viewed as a finite-state sequential machine, an automaton whose evolution is governed by linearly separable Boolean functions. From the former perspective, the original Hopfield network [3], designed to operate as a content-addressable memory, is a fully connected linear threshold model, but differs from that defined above in implementing an *asynchronous*, sequential update and imposing *symmetrical* couplings c_{ij}. The parallel-update (or *synchronous*) threshold model considered here has earlier antecedents [1,2].

The latter—Boolean network—perspective establishes a link with a seminal model introduced by Kauffman [4,5] nearly four decades ago to study the complex genetic regulatory system that guides cell differentiation in embryonic development. Although his initial studies were limited to low connectivity, the Kauffman model allows for all possible multicell interactions in a discrete logical sense: Units are updated in parallel, with the state of each unit at time $t+1$ being determined by a Boolean function of the states of its input units at time t. The logical function assigned to and implemented by a given unit is chosen randomly from the full set of Boolean functions. Restriction to the subclass of Boolean functions that are linearly separable allows for specialization to the threshold dynamics specified in Eq. (1).

As already suggested by the above description, the names of the elements comprising these network models are often tied to the scientific or real-world application envisioned. Thus, depending on problem domain,

$$\text{unit} = \text{node} = \text{point} = \text{vertex} = \text{site} = \text{spin} = \text{neuron} = \text{gene},$$

etc., and

$$\text{connection} = \text{input/output} = \text{link} = \text{edge} = \text{bond} = \text{coupling} = \text{axon/synapse} = \text{interaction},$$

etc.

III. DYNAMICAL BEHAVIOR: "FROZEN" VERSUS "CHAOTIC"

The bivalence of the Ising (or Boolean) variables assigned to the N units of the model means that there exist only 2^N different configurations in the state space of the network treated as a dynamical system. Consequently, the update rule (1) will inevitably lead the system into an attractor—a fixed point or a limit cycle—after a transient phase that is necessarily of finite (or zero) duration. This is obviously true for any deterministic sequential machine with a finite number of states, regardless of the specific update algorithm. The repertoire of long-term behaviors available to a given model, as represented by its characteristic set of attractors (also called "cyclic modes"), is a key determinant of the model's performance in either natural or technological contexts. For example, some aspects of fixed-point and cycling behaviors, often interpreted as the response of the network to stimuli expressed as initial conditions, may be of genetic, immunological, or neurocomputational interest within biology. In Kauffman's evolutionary model for cell differentiation, the total number of cyclic modes scales with the (highly limited) number of different cell types in living organisms. In neural-network models, fixed points and (relatively short) limit cycles can be considered as model analogs of active short-term memories or memory sequences [2,3,18]. Thus, when investigating the properties of complex dynamical networks, the acquisition of systematic information on long-term behavior assumes high priority, whether gained by analytical, statistical, and numerical methods (or a combination).

In the thermodynamic limit of asymptotically large N, useful statistical predictions for the dynamical motion corresponding to Eq. (1) can be obtained analytically, provided that the following holds true.

(i) The connectivity of the network (or equivalently its topology or "wiring diagram") is chosen randomly according to a specified probability distribution ϱ_k, where $k=k_i$ is the number of units j providing input to a generic unit i. In the model to be considered here, the initial connectivity of the network is such that all units i have the same in-degree $k_i = K$; i.e., every unit has exactly K incoming connections from K distinct input units j chosen with uniform probability from among the $N-1$ units other than i.

(ii) The network is sparsely connected (assured by $K \sim \ln N$ or less)

(iii) The weights c_{ij} of input connections to the processing units are chosen according to a given probability density distribution $\rho(c_{ij})$, with $c_{ij} \in \{-\infty, +\infty\}$.

The characteristic dynamical behavior of the model, stemming from Eq. (1), is conveniently analyzed in terms of the normalized Hamming distance between two system states $\sigma^{(1)}(t)$ and $\sigma^{(2)}(t)$, defined as

$$D_t = \frac{1}{2N} \sum_{i=1}^{N} |\sigma_i^{(1)}(t) - \sigma_i^{(2)}(t)| \tag{2}$$

and thus lying on the interval [0,1]. This quantity is of pivotal importance, in that its long-term behavior determines whether the system dynamics lies in the *ordered* or *chaotic* phase. Suppose the initial distance $D(t=0)$ has an infinitesimally small value. In the ordered (or "frozen") phase, the distance either remains small or eventually disappears for large times, whereas in the chaotic phase even an infinitesimally small initial distance will evolve into a finite distance ~ 1 at large t. Here we use the term "chaotic," even though a deterministic finite-state sequential machine cannot strictly exhibit chaos, since it is destined to enter a cyclic mode. However, it is well known that if the number N of units is asymptotically large, system trajectories can possess all of the statistical hallmarks of chaotic motion [20].

It is fruitful, both conceptually and in terms of potential applications, to characterize these two dynamical phases—ordered and chaotic—by their response to local damage, as produced by a reversal of the sign of one of the σ_i variables. The ordered phase, representing a stable condition of the system, is resistant to *damage spreading*: the wound does not spread; i.e., it remains confined. In the chaotic phase, on the other hand, the single-sign reversal may precipitate a cascade of sign reversals, eventually affecting $O(N)$ units; i.e., the damage spreads exponentially throughout the system. Following closely the techniques of the annealed approximation introduced by Derrida and co-workers [14–17], it was shown by one of us [9–11] in the late 1980s that for a symmetric distribution $\rho(c_{ij}) = \rho(-c_{ij})$ of the coupling coefficients, the equation of motion for the distance D_t can be written as a one-dimensional mapping

$$D_{t+1} = F(D_t) = 1 - \sum_{s=0}^{K} a_s \binom{K}{s} D_t^s (1 - D_t)^{K-s}. \tag{3}$$

For the threshold network models under study, the coefficients a_s are given directly by the K-dimensional probability integrals [11–13]

$$I_s^{(K)}(\rho, h) = \int \cdots \int dx_1 \cdots dx_K \rho(x_1) \cdots \rho(x_K) \times \theta(g(x_1, x_2, \ldots, x_K, h)), \tag{4}$$

where the $x_i \in \{-\infty, \infty\}$ are random variables representing the $c_{ij}\sigma_j$, θ denotes the Heaviside step function, and

$$\begin{aligned} g(x_1, \ldots, x_K, h) &= [(x_1 + x_2 + \cdots + x_s) + (x_{s+1} + \cdots + x_K + h)] \\ &\times [-(x_1 + x_2 + \cdots + x_s) + (x_{s+1} + \cdots + x_K)] \\ &= (x_{s+1} + \cdots + x_K + h)^2 - (x_1 + \cdots + x_s)^2. \end{aligned} \tag{5}$$

The integral $I_s^{(K)}(\rho, h)$ specifies the probability that a sign reversal of s randomly chosen input variables σ_j at time t will *not* affect the output state of the system at the next time step, $t+1$. We note that for the trivial case $s=0$, the integral $I_0^{(K)}(\rho, h)$ is unity.

At this point, comparison with the Kauffman model is instructive [12,21]. In this model it is customary to suppose that all units have the same number K of inputs (same in-degree), just as in the initial connectivity specified for our model. The key distinction is that the processing units in the Kauffman model have access to *all* of the 2^N possible Boolean state-transition functions. The present model, based on linear threshold updating of the state, admits only the relatively small *subclass* of linearly separable Boolean functions.

More specifically, in the Kauffman model, the state-transition functions are chosen randomly from the full Boolean class, but with a bias such that they yield 0 and 1 with respective probabilities $1-p$ and p. Consequently, in this model the coefficients a_s introduced above, with the exception of $a_0 = 1$, take the *same* value $2p(1-p)$, independently of s. By contrast, for the linear threshold model [9], Eq. (1) informs us that the coefficients a_s depend on the in-degree s, and indeed also on the chosen distribution $\rho(c_{ij})$ of the connection weights and the threshold parameter h.

Equation (3) has a trivial fixed point $D \equiv 0$ which is stable if and only if the slope of $F(D_t)$ evaluated at $D=0$ satisfies

$$\left. \frac{dF}{dD_t} \right|_{D_t \equiv 0} = K[1 - I_1^{(K)}(\rho, h)] \leq 1. \tag{6}$$

In general, this implies that a small initial distance decays exponentially to zero. However, at the critical point corresponding to equality in condition (6), the behavior is special, with the distance tending logarithmically to zero [12] $(\sim 1/\ln t)$. Inspection of the above condition shows that the critical behavior is determined by the first-order coefficient a_1 of expansion in Eq. (3), hence only on

$$I_1^{(K)}(\rho, h) = \int \cdots \int dx_1 \cdots dx_K \rho(x_1) \cdots \rho(x_K) \times \theta((x_2 + \cdots + x_K + h)^2 - x_1^2). \tag{7}$$

This is natural: if the fixed point $D \equiv 0$ is unstable against single spin flips, it is unstable against multiple flips. On the other hand, if the initial distance $D_{t=0}$ for Eq. (2) evolves to a finite distance $D^* \neq 0$, all coefficients a_s of the expansion in Eq. (3)—i.e., all of the probability integrals $I_s^{(K)}(\rho, h)$—are needed for an analytic prediction of the corresponding nonzero fixed points D^*.

We will establish that the formal analysis based on the annealed approximation may be extended not only to the case in which the in-degree k_i is variable, but also to cases in

which the connection weights may be chosen from a continuum, as well as from a discrete set of values such as $\{-1,0,+1\}$.

IV. VARIABLE CONNECTIVITY THROUGH DILUTION

Let us now consider in more depth an algorithm that (i) introduces variable in-degrees through dilution of a previously constructed homogeneous network and also (ii) provides nontrivially for variable connection strengths.

First, we assemble ("wire up") the network randomly, just as before, such that each unit receives the same number K of inputs. Second, we perform a random deletion of a fraction $1-\zeta$ of the $i\rightarrow j$ connections made in the first step. The in-degree k of a given unit may now vary between 0 and K, and the mean connectivity of the networks is

$$\bar{K} = \zeta K. \tag{8}$$

Since the number N of units is asymptotically large, and hence also the number NK of connections, and since K is also to be considered large (but much smaller than N), the in-degree distribution ϱ_k of the diluted network, while strictly binomial, is effectively Poissonian with mean $\bar{K}$.

In a final step, the strengths c_{ij} of the surviving connections are chosen based on a symmetric distribution $\rho_0(x)$ (which we call the base-line distribution). The nonzero couplings c_{ij} are determined by sampling the distribution $\rho_0(x)$ with weight ζ. The pattern of connectivity and couplings characterizing the ensemble of diluted networks is represented analytically by the probability density distribution

$$\rho(x) = \zeta\rho_0(x) + (1-\zeta)\delta(x). \tag{9}$$

Obviously, the in-degree distribution ϱ_k is unaffected by this step and remains essentially Poissonian. Substituting the distribution (9) into the integral (7), we have, with a shift of the summation index $k\rightarrow k+1$,

$$I_1^{(K)}(\rho,h) = (1-\zeta) + \sum_{k=0}^{K-1} \binom{K-1}{k} \zeta^{k+1}(1-\zeta)^{K-1-k} I_1^{(k+1)}(\rho_0,h), \tag{10}$$

where $I_1^{(k+1)}(\rho_0,h)$ is given by Eq. (7) with $\rho=\rho_0$ and K replaced by $0\leq k\leq K-1$. Inserting this result into relation (6) for the case of equality, we obtain

$$K\left[\zeta - \sum_{k=1}^{K} \binom{K-1}{k-1} \zeta^{k}(1-\zeta)^{K-k} I_1^{(k)}(\rho_0,h)\right] = 1. \tag{11}$$

For fixed parameters K and h, Eq. (11) now serves to determine the critical dilution $1-\zeta_c$ above which the system belongs to the stable, ordered phase. The corresponding *critical mean connectivity* is then given by $\bar{K}_c=\zeta_c K$.

V. PUSHING THE ENVELOPE OF STABILITY

The algorithm we have introduced allows for gross control over the network's connectivity, or topology, through the choices made for the dilution parameter $1-\zeta$ and the connectivity parameter K (which becomes the maximum in-degree). Furthermore, it allows for diversity of the connection weights c_{ij} through specification of the distribution of coupling strengths assigned to the surviving connections.

Within the annealed approximation, we have shown explicitly how the boundary between the chaotic and ordered regimes, and hence the extent of the stable regime, depends on the assumed distribution $\rho(x)$. More specifically in terms of our statistical prescription for construction of the diluted network with varying connection weights, we have shown how the boundary between stability and instability depends on the choice of the base-line distribution $\rho_0(x)$, the dilution parameter $1-\zeta$, the connectivity parameter K, and the threshold parameter h.

Based on our results, it is in fact both practical and possible to gain useful theoretical insights by applying the annealed approximation to the case in which the in-degree is variable from one node (unit) to another (cf. Ref. [22]). Moreover, our approach is also well suited to the treatment of networks in which the nonzero connection strengths are not restricted to a discrete set of values (as in Refs. [22,23]), but instead may belong to a continuum. We shall now make use of this flexibility to explore the relative stability against chaos, or damage spreading, of the dynamics of random threshold network models corresponding to different choices of the base-line distribution $\rho_0(x)$ entering Eq. (9). These choices, all symmetrical under $x\rightarrow -x$, include the following: (i) the bivalent "Dirac" distribution

$$\rho_0(x) = \frac{1}{2}[\delta(1-x) + \delta(1+x)]; \tag{12}$$

(ii) a uniform probability density on the interval $[-1,1]$,

$$\rho_0(x) = \frac{1}{2}\theta(x)[1-\theta(x)]; \tag{13}$$

and (iii) the Gaussian distribution

$$\rho_0(x) = \frac{1}{\sqrt{\pi}} e^{-x^2}. \tag{14}$$

To these we add (iv) a power-law distribution, given by

$$\rho_0(x) = \frac{1}{2}\frac{1-\alpha}{|x|^{\alpha}} \tag{15}$$

on $-1<x<1$ and vanishing otherwise, with $0<\alpha<1$.

All four of these base-line distributions $\rho_0(x)$ are properly normalized, such that $\int_{-\infty}^{\infty}\rho_0(x)dx=1$. (Although the power-law distribution is singular at the origin, it is integrable.) Moreover, all four choices of $\rho_0(x)$ [and hence the overall distribution $\rho(x)$ of Eq. (9)] are even in the random variable x, which means that we assume equal probability of excitatory or inhibitory connections. However, our current analysis anticipates treatment of an arbitrary real-number threshold parameter h.

Consider now the k-dimensional probability integrals $I_1^{(k)}(\rho,h)$ defined by Eq. (7) with K rewritten as k. These integrals, with k running from 1 to K and $\rho_0(x)$ substituted for $\rho(x)$, are needed to explicate the stability condition and

determine the critical boundary in the dynamical phase diagram of the diluted system through Eq. (11). For standard probability density distributions $\rho_0(x)$, these integrals may be evaluated in closed form by making use of the recursion relation

$$I_1^{(k+1)}(\rho_0,h) = \int dx\, \rho_0(x) I_1^{(k)}(\rho_0,x+h), \tag{16}$$

which follows directly from the definition (7) of the probability integrals (with $K \to k+1$).

For the first three base-line distributions listed above, the following analytical expressions have been obtained by a process of induction. The details of the derivations are lengthy and tedious and will not be reproduced here; the results of a more general analysis of the probability integrals entering Hamming-distance dynamics will be published elsewhere in a dedicated article.

(i) *Bivalent Dirac distribution*:

$$I_1^{(k)}(\rho_0,h) = 1 - \frac{1}{2^k}\binom{k}{(k+h)/2} \quad (\text{if } k+h \text{ is even})$$

$$= I(k-1,h) \quad (\text{if } k+h \text{ is odd}). \tag{17}$$

Upon inserting this result into Eq. (24) below, we reproduce a result derived by Rohlf and Bornholdt [22] using combinatoric arguments.

(ii) *Uniform density*:

$$I_1^{(k)}(\rho_0,h) = \frac{1}{2^{k-1}k!}\sum_{l=-k}^{k} c_l^k (h-l)_+^k, \tag{18}$$

wherein the factor bearing the + subscript is evaluated as given if $h-l$ is positive; otherwise, it is set equal to zero. The coefficients c_l^k are then given by the two-dimensional recursion relation

$$c_l^{k+1} = c_{l+1}^k - c_{l-1}^k, \quad l = -k, \ldots, +k, \quad k = 1, \ldots, N, \tag{19}$$

where $c_{\pm 1}^1 = -1$ and $c_0^1 = 2$. This result has been published previously by one of us in Ref. [9].

(iii) *Gaussian distribution*:

$$I_1^{(k)}(\rho_0,h) = 1 - \frac{2}{\pi}\int_{|h|/\sqrt{k}}^{\infty} e^{-x^2} \phi\left(\frac{x}{\sqrt{k-1}}\right) dx, \tag{20}$$

where $\phi(x)$ is the error function. For $h=0$, this formula reproduces a result obtained by Derrida [16].

For the power-law distribution (15), the integrals $I_1^{(k)}(\rho_0,h)$ cannot be calculated analytically for arbitrary values of k. However, the required probability integrals for this case can be evaluated numerically by a Monte Carlo algorithm. Indeed, although the above analytical formulas are available for calculation of the integrals $I_1^{(k)}(\rho_0,h)$ for the other three distributions, the Monte Carlo technique is more convenient for their numerical computation; accordingly, it has been used in all cases to determine the data for $I_1^{(k)}(\rho_0,h)$ versus k plotted in Figs. 1 and 4, on which our evaluation of critical mean connectivity is based.

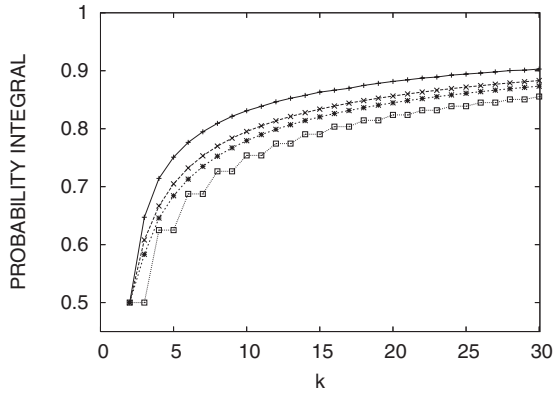

FIG. 1. Results for the probability integrals $I_1^{(k)}(\rho_0,h=0)$ corresponding to four different base-line probability density distributions $\rho_0(x)$, plotted versus in-degree index k. Key, reading from bottom to top: Dotted curve with squares: bivalent Dirac distribution. Short-dashed curve with stars: uniform distribution. Long-dashed curve with crosses: Gaussian distribution. Solid curve with pluses: power-law distribution with $\alpha=2/3$.

Evaluation of the integrals $I_1^{(k)}(\rho_0,h)$ simplifies considerably for vanishing threshold parameter h. All numerical results presented here refer to this case. Probability integrals for the four base-line distributions are shown in Fig. 1 as functions of the in-degree index k. Figure 2 collects plots of the line of critical mean connectivity $\bar{K}_c$ as a function of the upper bound K on the in-degrees assigned to the units (identical with the initial uniform in-degree). The different curves correspond to the four different choices (12)–(15) for the base-line distribution $\rho_0(x)$. The corresponding chaotic regime lies above each curve. The lowest curve (least stable case) gives $\bar{K}_c$ for the bivalent Dirac distribution. With increasing K, the critical mean connectivity slowly increases toward an asymptotic value $\bar{K}_c^{\infty} = 1.848\,87$ (determined as described below). The same general behavior is seen for the other distributions examined. However, the curves for the

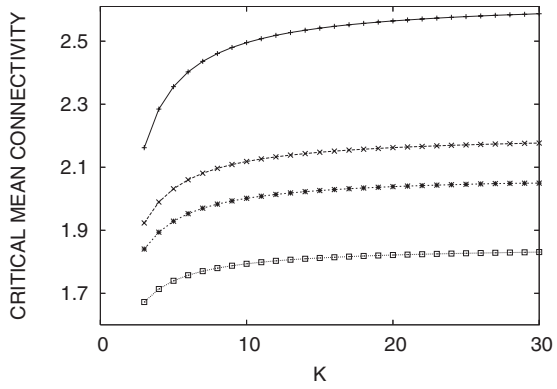

FIG. 2. Critical mean connectivity $\bar{K}_c$ as a function of connectivity parameter K for four choices of the base-line probability density distribution $\rho_0(x)$. Key, reading from bottom to top: Dotted curve with squares: bivalent Dirac distribution. Short-dashed curve with stars: uniform distribution. Long-dashed curve with crosses: Gaussian distribution. Solid curve with pluses: power-law distribution with $\alpha=2/3$.

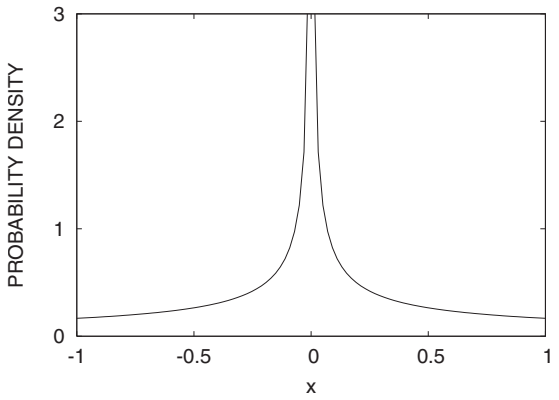

FIG. 3. Power-law density distribution $\rho_0(x)=(1-\alpha)/2|x|^{\alpha}$, plotted for $\alpha=2/3$.

uniform and Gaussian choices show successively greater stability, with shrinking chaotic regimes and asymptotic values of $\bar{K}_c^{\infty}=2.074$ and 2.206, respectively. Note that the latter critical value for the Gaussian choice has already been reported in 1987 by Derrida (see Ref. [16]). Results are also included for the power-law distribution (15) plotted in Fig. 3, taking $\alpha=2/3$ for the *control parameter* that is available for this choice of distribution. In this case the asymptotic critical mean connectivity is found to be $\bar{K}_c^{\infty}=2.63$, substantially larger than the values attained for the other three distributions.

The asymptotic values quoted for $K\to\infty$ are easily calculated directly by eliminating ζ in favor of the mean connectivity $\bar{K}$. Substituting $\zeta=\bar{K}/K$ into Eq. (10), we have

$$I_1^{(K)}(\rho,h)=\left(1-\frac{\bar{K}}{K}\right)+\sum_{k=0}^{K-1}\frac{(K-1)!}{k\,!\,(K-k-1)!}\times\left(\frac{\bar{K}}{K}\right)^{k+1}\left(1-\frac{\bar{K}}{K}\right)^{K-1-k}I_1^{(k+1)}(\rho_0,h)$$
$$=\left(1-\frac{\bar{K}}{K}\right)+\sum_{k=0}^{K-1}\left[\frac{(K-1)!}{(K-1-k)\,!\,K^k}\right]\frac{\bar{K}}{K}\frac{\bar{K}^k}{k!}\times\left[\left(1-\frac{\bar{K}}{K}\right)^{K}\right]\left[\left(\frac{K}{K-\bar{K}}\right)^{k+1}\right]I_1^{(k+1)}(\rho_0,h). \tag{21}$$

In the thermodynamic limit where $K\sim\ln N$ and $N\to\infty$, the factor in the second set of square brackets defines the exponential $e^{-\bar{K}}$, while the those in the first and third reduce to unity. Reduction of the latter factors proceeds as follows. The first can be rewritten as

$$(K-1-k+1)(K-1-k+2)\cdots(K-1-k+k)K^{-k}. \tag{22}$$

The factorial $k!$ appearing in the denominator of the sum over k quenches the contributions from all k of size comparable to K, so that in the limit $K\to\infty$, expression (22) may be replaced by $K^kK^{-k}=1$. For the factor in the third set of square brackets, we observe that $\bar{K}$ is necessarily a small number in the region of the boundary between ordered and chaotic phases, so that this factor reduces trivially to unity at asymptotically large K.

Thus we arrive at

$$I_1^{(K)}(\rho,h)=\left(1-\frac{\bar{K}}{K}\right)+\frac{\bar{K}}{K}e^{-\bar{K}}\sum_{k=0}^{K-1}\frac{\bar{K}^k}{k!}I_1^{(k+1)}(\rho_0,h). \tag{23}$$

One recognizes that the manipulations leading to this result recapitulate steps made in deriving the approximation of a Binomial distribution by a Poisson distribution. The critical stability condition for $\bar{K}$, corresponding to condition (11), but for asymptotically large K, is now given by

$$\bar{K}\left(1-e^{-\bar{K}}\sum_{k=0}^{\infty}\frac{\bar{K}^k}{k!}I_1^{(k+1)}(\rho_0,h)\right)\leq 1, \tag{24}$$

so that the critical value $\bar{K}_c$ of $\bar{K}$ is determined by a nonlinear algebraic equation. The series appearing in the left-hand side of Eq. (24) converges rapidly.

The principal findings of this numerical investigation may be summarized as follows. Of the probability density distributions selected for comparison, the power-law choice, with $\alpha=2/3$, endows the system with the greatest stability or robustness, in the sense of producing the highest critical mean connectivity $\bar{K}_c$ for a given upper bound K on the in-degree assigned to the units. Moreover, the stability associated with the power-law distribution can be tuned. As α is decreased, the chaotic phase expands at the expense of the frozen phase. The limiting distribution for $\alpha\to 0$ is equivalent to the uniform choice (13) and accordingly yields the *same* $\bar{K}_c$ for given K. On the other hand, the stable domain can be expanded without limit as the parameter α is increased toward its upper limit of unity. While stability can certainly be enhanced in this way, it eventually proves counterproductive: For $\alpha\to 1$, the distribution becomes a spike at $x=0$, all the couplings c_{ij} are zero, and the network is completely disconnected.

It is well to emphasize that the power-law distribution (15) stands apart from the other three distribution functions considered in that it contains the adjustable parameter α and hence represents a family of distributions rather than a single choice. One might similarly generalize the Gaussian choice (14) to a family of properly normalized Gaussians,

$$\rho_0(x)=\frac{1}{\sqrt{\pi\beta^2}}e^{-x^2/\beta^2}. \tag{25}$$

However, it is readily shown that the probability integrals $I_1^{(k)}(\rho_0,h)$ for this distribution are independent of the parameter β and hence invariant under this generalization.

Figures 4 and 5 provide supplementary results for probability integrals and critical mean connectivity values associated with the power-law distribution. Results are shown for parameter values $\alpha=0,1/6,2/6,3/6$ as well as 2/3. (The required numerical computations for larger α values become excessively demanding, especially at large values of K.)

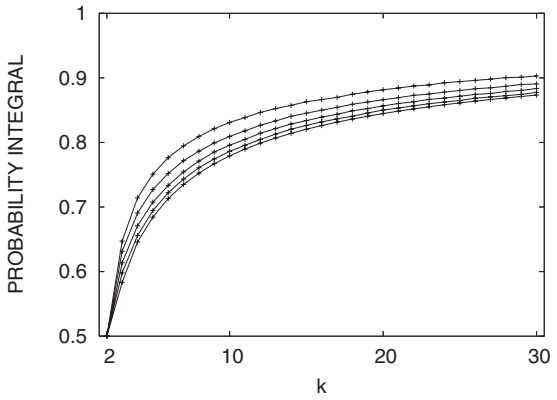

FIG. 4. Results for the probability integrals $I_1^{(k)}(\rho_0, h=0)$, plotted versus in-degree index k for several values of the power α specifying the power-law distribution (15). From bottom to top, the curves correspond to $\alpha=0$, 1/6, 2/6, 3/6, and 4/6.

VI. DISCUSSION

We begin the discussion of the meaning, implications, and relationships of the results of Sec. V with a simple qualitative explanation of the differing degrees of stability endowed by the different choices of base-line connection-strength distributions studied numerically. We then relate our findings, insofar as possible, to the results of other studies of the dynamical stability of randomly assembled threshold networks, as measured by their susceptibility to damage spreading. Since the formation of the network models studied here involves pruning of connections initially present, we call attention to situations in neurobiology and neural modeling where processes of synaptic elimination may play important roles.

A. Qualitative interpretation of principal findings

It is well known from earlier work (e.g., Ref. [11]) that in the absence of dilution ($\zeta=1$), (i) a smaller value of the connectivity parameter K favors stability and disfavors chaos and (ii) no disordered phase can occur for $K<3$. It is also known that at a given, finite value of the dilution ($0<1-\zeta<1$), property (i) remains true, but fluctuations of the in-degrees assigned to the units (which can range from 0 to K) permit a chaotic region to exist for mean connectivity $\bar{K}=\langle k\rangle$ *less than* 3. We note, *inter alia*, that the mean connectivity always exists as a meaningful quantity in our models.

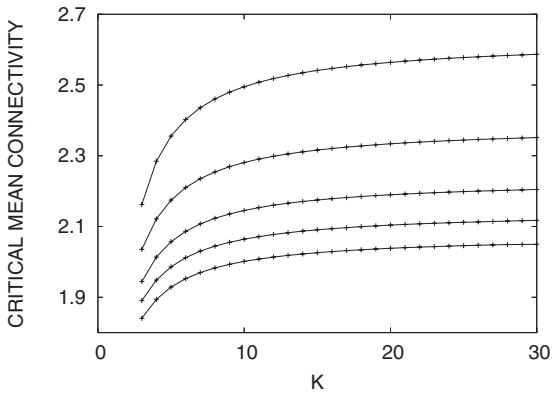

FIG. 5. Critical mean connectivity $\bar{K}_c$ as a function of connectivity parameter K for several values of the power α specifying the power-law distribution (15). From bottom to top, the curves correspond to $\alpha=0$, 1/6, 2/6, 3/6, and 4/6.

Next we remark that although in principle the base-line distribution $\rho_0(x)$ can produce further dilution beyond the fraction $1-\zeta$ by assigning zero strength to some of the remaining connections, in practice the effect will be of measure zero for the distribution functions we have employed. On the other hand, to the extent that a given choice of $\rho_0(x)$ assigns *small* weights to a significant fraction of the surviving links, the effectiveness of these links in spreading damage will be correspondingly reduced. Considered from the viewpoint of *topology*, the mean connectivity is decreased, with a corresponding retreat of the chaotic domain in the dynamical phase diagram. Considered from the viewpoint of *connection strengths* (which in fact embraces the topology), the mean absolute strength $|\bar{c}|$ of connections that survive pruning is correspondingly weakened. Either perspective offers some *qualitative* insight into the ordering of stability for the four distributions studied in Sec. V, as quantified in Figs. 2 and 5, but it must be expected that significant features of the problem are missed in focusing on such mean values, as indicated in the next paragraph.

For the binary Dirac distribution (12), the weights of the existing connections all have the same absolute value $|\bar{c}|$ of unity. For the uniform distribution (13), the mean absolute value $|\bar{c}|$ is reduced to 1/2. For the Gaussian distribution (14), $|\bar{c}|$ is further suppressed, the connection strengths close to zero having higher probability. The power-law case is more interesting. As the parameter α runs through the range (0,1), the power law yields a mean absolute connection weight that interpolates smoothly between limiting values of 1/2 (the same as for the uniform distribution) and 0, as $\alpha\to 0$ and $\alpha\to 1$, respectively. The mean value of $|c|$ can also be driven to zero by adopting the parametrized Gaussian distribution (25) and taking the width parameter β to zero. However, in contrast to the behavior found for the power-law distribution under variation of the parameter α, the Gaussian choice (25) has the property that the dynamical stability of the network remains unaffected as β is varied, the critical line being independent of β.

B. Relationships to prior work

Three prior investigations [22–24] of the competition between chaos and order in complex networks are sufficiently recent and relevant to warrant comparison with our analysis. However, these earlier studies differ from the present work in their focus on the effects of network topology, examining the dynamical implications of variable in-degree k corresponding to an assumed distribution ϱ_k, but not exploring the effects of variable magnitudes of the nonzero connection strengths. References [22,23] address the issues of stability and damage spreading within the model class of randomly assembled threshold networks, while Ref. [24] determines conditions for dynamical robustness of random Boolean networks.

Although the models studied in Refs. [22,23] are similar to those we have considered, there are some crucial differences. In the cited works, the coupling strengths c_{ij} are restricted to the discrete set of values $\{-1,0,+1\}$ and the values $-1,+1$ are assigned with equal probabilities. The fraction of null connections ($c_{ij}=0$) is not specified explicitly, but is constrained by specification of a mean connectivity (mean in-degree) parameter $\bar{K}$ and by other assumptions on the in-degree distribution. Our more general description allows the couplings c_{ij} to take on any real values. Within the framework of our models, formulated in terms of the probability density distribution $\rho(x)$ of connection strengths, the models of Refs. [22,23] correspond to Eq. (9) with the bivalent Dirac choice (12) taken for $\rho_0(x)$. The quantities corresponding to the integrals $I_1^{(k)}(\rho,h)$ of our treatment [denoted by $p_s(k)$ in Refs. [22,23]] are determined by combinatoric arguments that have no practical extension to the more general connection-strength probability density distributions considered in our work.

In the models analyzed in Refs. [22,23], there is no upper limit on the in-degree of a given unit, whereas in our models the in-degree is bounded by the parameter K. This is an important distinction. It implies that a useful comparison can only be made by going to the thermodynamic limit for K within the present approach [and, of course, only for the bivalent Dirac choice of $\rho_0(x)$]. Thus, we may compare the critical connectivity $K_c=1.849\pm0.001$ determined in Ref. [22] with the asymptotic mean connectivity $\bar{K}_c^{\infty}=1.848\,87$ found in Sec. V. It is not surprising that these values agree, since they are in fact computed from the same formula, obtained by substituting the bivalent Dirac distribution into the integrals entering Eq. (24).

The work of Aldana and Cluzel [24] is of seminal significance in demonstrating, for the iconic Kauffman model, that a scale-free (power-law) choice $\varrho_k\sim k^{-\gamma}$ for the *in-degree distribution* can yield greatly enhanced *robustness* relative to that of networks with random topology—i.e., wired up as in our models prior to dilution. Robustness is defined as the fraction of the range $[0,1]$ of the bias parameter p over which networks display robust (i.e., ordered, not chaotic) behavior.

In a sense this finding is mirrored in our demonstration, within the more restricted setting of linear threshold networks, that a power-law *density* distribution of (nonzero) *connection strengths* can yield enhanced stability compared to bivalent Dirac, uniform, and Gaussian forms. The competition between ordered and chaotic phases can be tuned by adjusting the index α specifying the power-law distribution (15). In both model studies, the introduction of heterogeneity into the structural characterization of a complex network model through a power-law distribution provides for greater stability than can be achieved with a more homogeneous design.

However, we should emphasize that despite this commonality, the correspondence is indirect, and essential distinctions must again be drawn. The first of these involves the nature of the parameter domains (the dynamical phase diagrams) being explored. The dynamical behavior of the Boolean models was investigated by Aldana and Cluzel either in the phase plane $(p,\bar{K})$ (appropriate to the random topology) or in the phase plane (p,γ) (appropriate for the scale-free topology). On the other hand, our work is concerned with the dynamical behavior of threshold networks in the phase plane $(\bar{K}_c,K)$, or equivalently (ζ,K), for various choices of the connection-strength distribution. The parameter ζ has no counterpart in the Boolean models, so the two studies actually address different aspects of the stability. A more apt comparison could be made if the dynamics of the threshold network model were examined for a range of values of the threshold parameter h, which, like p in the Boolean case, provides a single parameter measuring the probability that an arbitrary unit i will become active, $\sigma_i=+1$. From prior comparisons of Boolean and threshold models (see, e.g., Ref. [12]), one may expect corresponding behavior. Specifically, one may expect greater robustness of performance in terms of an expansion of the range of h over which the threshold-network system displays ordered behavior, when a scale-free in-degree distribution ϱ_k is used in place of the conventional homogeneous random topology. [We note here that the probability integrals $I_1^k(\rho,h)$ increase monotonically with the threshold parameter h.]

The second important distinction stems from the fact that the power-law, or "scale-free," form plays a different role in the present work than it does in the study of Aldana and Cluzel or the investigations of Refs. [22,23]. These latter analyses follow the trend of the majority of current studies of complex networks, in which topological considerations are paramount. In particular, Albert and Barabási [8] have collected empirical evidence demonstrating that in many large networks observed in physical, biological, economic, and social systems, the degree distribution ϱ_k (or the in-degree and out-degree distributions if they differ) obeys a power law at large k. Furthermore, they have shown that such a behavior may result from regular growth of the number of nodes (units), followed by preferential attachment to nodes of high degree. Based on the work of Aldana and Cluzel for the Kauffman model, one may reasonably expect that also in the case of threshold networks, the choice of an (in-) degree distribution with a power-law tail will promote stability of dynamical operation. A natural way to introduce the *next* layer of complexity is to assign strengths of various magnitudes to the nonzero connections. That is what we have done, while diluting an initial topology (wiring diagram) that is homogeneously random.

It should also be noted that the algorithm for network construction we have adopted is based on a different view of the evolution of networks than that of Albert and Barabási; we implement pruning of connections rather than growth, while allowing for variance of connection strengths. To reiterate: First, all possible connections between the N processing units are made, and links are then deleted at random until a fraction ζ of the original NK links is left. These ζNK nonzero connections are assigned positive and negative strengths symmetrically according to the power-law (or scale-free) distribution (15). We have found that for sufficiently large values of α, the inhomogeneous distribution of connection strengths arising from this algorithm leads to greater stability than can be attained with more homogeneous distributions and that the unstable chaotic phase shrinks indefinitely as the

power α approaches its upper bound of unity. To explain the relative stabilities associated with the four choices (12)–(15), it was argued that in determining the boundary between ordered and chaotic phases, the connections having very small absolute strength are equivalent to an additional fraction of zero connections. In general, a reduction in the mean number of input connections per unit promotes stability; however, the details of the phase diagram will also depend both on the variance in the in-degree and the variance in the absolute connection strength. It is also worth noting (again) that pushing toward the limit $\alpha \to 1$ may not be advantageous in practice, since its effect is ultimately to trim out all connections.

The importance of the in-degree variance for network behavior was stressed in Ref. [24]. Although the mean connectivity $\bar{K}$ is a meaningful guide in the case of the homogeneous random topology, this quantity has little meaning for the scale-free topology. In the former case, the degree distribution becomes Poissonian for large $\bar{K}$, and hence the variance coincides with $\bar{K}$. In the latter case, however, the variance is divergent for $\gamma \leq 3$ in the relevant thermodynamic limit, so that the mean connectivity (mean in-degree) is no longer a useful concept. We point out that in the models studied here, $\bar{K}$ remains meaningful, since by construction it is bounded by K, which is either finite or at worst $O(\ln N)$ for large N.

Because of the differing roles of the power-law distribution in the present work and that of Refs. [8,22–24], it is to be expected that the interesting ranges of the power-law exponent are different. This is highlighted by our use of the symbol α for the power-law index in Eq. (15) rather than the more conventional notation [8,23,24] γ. In their studies of Boolean nets, Aldana and Cluzel found that scale-free topology with $\gamma > 2.5$ yields robust dynamics for any value of p, with the transition from order to chaos occurring when the γ value is reduced to $\gamma \approx 2$, depending mildly on p. These authors cite empirical evidence that real intracellular networks are characterized by γ values in the range [2,2.5] they predict for the transition region. In the threshold network models considered here, the values α are restricted to the range (0,1) to ensure normalization of the distribution (15).

In concluding this discussion, we would like to emphasize that when the scale-free form $\varrho_k \sim k^{-\gamma}$ is employed as a representation of the degree distribution [8,22–24], what is important is its behavior at *large* k—i.e., its slow falloff compared, say, to a Poisson or Gaussian distribution. Indeed, its behavior at very low k, especially $k=0$, is clearly not meaningful in this application. (Accordingly, Nakamura [23] starts the "scale-free" power-law form at $k=1$; he also imposes a cutoff at large k.) On the other hand, when the power-law form is used to represent the probability density distribution of connection strengths, what is *most* important is its behavior at *low* $|c_{ij}|$, as argued above. In neither case is one truly dealing with a scale-free distribution, as some scale must intervene physically at either low or high values of the relevant variable (or both).

C. Synaptic deletion in neurobiology and neural modeling

Finally, let us turn to the possible biological or practical significance of the findings of the present study with respect to the dynamical stability of threshold networks. One question to be dealt with is the relevance of the class of network models we have investigated to real-world complex networks—specifically, the relevance of the algorithm of random deletion of connections that underlies the creation of these models.

It is a well-known phenomenon in brain development that an early phase of overproduction of synaptic connections is followed by massive pruning of synapses [25–32]. Evidence for synaptic elimination is found, for example, in the visual cortex, association areas, and the voluntary motor area, as well as at neuromuscular junctions. In humans, for example, synaptic density increases linearly during fetal and postnatal development, reaching a maximum around age 2–3 and remaining stable at 150%–200% adult levels until about age 5. At that point a process of vigorous synaptic pruning begins, synapses being eliminated until the density stabilizes at adult levels around the time of puberty [37].

The processes of synaptic reorganization that take place in learning and development are largely unknown. In the absence of data showing correlations between localized neural activity and persistence or extinction of synaptic connections, it is reasonable to adopt a prescription of random deletion, as in our model. On the other hand, if synaptic reorganization, including elimination of connections, is to have some utility for an organism or in a device, the process must involve a systematic component, for which empirical evidence does exist in some cases.

One such case may be established in observation and analysis of the developmental stages of the frog neuromuscular junction [33]. In early stages, each muscle fiber is innervated by multiple motor neurons, but after development is complete each fiber is controlled by a single motor axon. During development, it is observed that active neurons maintain small motor units (in terms of muscle fibers controlled), whereas other evidence suggests that activity drives competition at the neuromuscular junction. The paradox created by these findings has been resolved in a dynamical model [34] of synaptic competition that takes into account the global redistribution of synaptic resources as local competition eliminates axonal connections at individual neuromuscular junctions, while providing an explanation of the size principle [35] of muscle fiber recruitment in the adult system.

It may be expected that the tasks of memory storage and retrieval call for deletion strategies rather different from those that are optimal for muscular action. In this respect we note that there has been significant theoretical work on the effect of synapse elimination on capacity measures in associative memory models [36–38]. Sompolinsky [36] and later Chechik, Meilijson, and Ruppin [37] have argued that when metabolic resources are not constrained, no deletion strategy can yield better performance than the intact network. However, the latter authors have shown that when metabolic energy resources are limited in terms of the number of synapses or total absolute synaptic strength, memory performance (measured by patterns stored per synapse) is maximized if synapses are first overproduced and then pruned by an optimal minimal-value deletion strategy (trimming out all synapses of magnitude smaller than a given value). More recently, Mimura, Kimoto, and Okada [38] have studied the

effect on synapse efficiency of different pruning algorithms: namely random deletion, synapse clipping, minimal-value deletion, and compressed deletion. In their work, synapse efficiency is defined as the storage capacity normalized by the "connection rate" (a single number representing the out-degree).

These disparate examples suggest that different realizations of systematic synapse deletion will be favored in different neurobiological settings. Accordingly, generic studies of networks subjected to random deletion of connections, such as that presented here, will remain of value in providing a base-line case.

D. Directions for future work

The present study of the dynamical stability of threshold networks has been based on a rather simple topology-generating algorithm and several options for subsequent probabilistic determination of the strengths of surviving connections. The topology-generating algorithm, which involves random dilution of connections after first wiring up the network with uniform in-degree K, has been motivated in part by the evolution of synaptic connections in early neural development in vertebrates. The critical dynamics of the network models thus created has been explored by following the evolution of the Hamming distance between network replicas within the annealed approximation.

Further work along similar lines may serve to remove some of the limitations of the present treatment and/or explore alternatives to the connection-pruning scenario. Naturally there are many directions in which one could proceed toward a more realistic description, depending on the specific, real-world application that is envisioned. Here we mention three projects, one of which is currently in progress.

(i) In the models studied here, the processes of topology generation (characterized by the final in-degree distribution ϱ_k) and connection-weight assignment [characterized by the probability density $\rho_0(x)$] are uncorrelated. A more realistic description will require the introduction of correlations suited to the anticipated application. For example, in the case of a neural network, one could argue (at least if resource constraints on synaptic enhancement are ignored) that connections with weak weights should have a higher probability of vanishing. This could be enforced in the present framework by implementing a final dilution step to trim out the weak links.

(ii) In the work reported here, we have studied the relative dynamical stability of network models for different choices of the probability density $\rho_0(x)$ of the strengths of connections, the in-degree distribution being fixed and essentially Poisonnian. To gain a more complete understanding of the network properties contributing to stability, a complementary study should be performed in which the in-degree distribution ϱ_k is varied at fixed $\rho_0(x)$, for each choice of $\rho_0(x)$ considered in the present work. Preliminary results from such a study, in which Poisson, exponential, and power-law distributions are considered for ϱ_k, point to a clear advantage for the power-law form in promoting stability. This finding is what could be expected from the qualitative argument for the favorability of the power-law form given in Sec. VI A and from the discussion of the Boolean-network studies of Aldana and Cluzel [24] in Sec. VI B.

(iii) The topology-generating algorithm we have employed features dilution of connections in a preformed network. A mirror-image scenario, in which pruning in replaced by growth of new connections, is equally worthy of study along the same lines, as is a scenario in which connections are grown "from a blank slate." In either of these alternative scenarios, overt attention to resource constraints may be necessary, depending on the application.

ACKNOWLEDGMENTS

K.E.K. is indebted to B. Derrida for illuminating discussions of this class of problems in the late 1980s and for specific advice that has been crucial to the present work as well as that reported in Refs. [9–13]. Early discussions with G. Senger on analytical aspects of the problem are also appreciated. K.E.K. thanks P. Martin, S. Charpentier, and O. Machon of the Université du Littoral de Dunkerque for computational assistance, as well M. Ayachi of the Faculté des Sciences of the University of Monastir for helpful insights into the analytical derivation of the probability integrals. The research reported here was supported in part by the McDonnell Center for the Space Sciences. J.W.C. would like to acknowledge partial support from FCT POCTI, FEDER in Portugal through grants to the Centro de Ciencias Mathematicas, University of Madeira, in connection with the Madeira Math Encounters.

APPENDIX

The use of one-dimensional mappings of the kind (3) to update the time evolution of the Hamming distance between two replicas [(1) and (2)] of a Boolean or neural network of binary units dates from the pioneering work of Derrida and co-workers [14–17] some two decades ago. Accordingly, it is worthwhile to recapitulate briefly the basis of such distance equations. In essence, but with certain elective modifications to mesh with the current application, we follow the derivation presented by Derrida in Ref. [16].

First, there is the assumption of sparsely connectivity as made in item (ii) of Sec. III. Under this assumption, the Hamming-distance dynamics of the of the quenched model, for which the coupling strengths c_{ij} are randomly chosen at the initial time and kept fixed thereafter, is reproduced by that for the annealed model, in which the c_{ij} are chosen afresh at each time step in accordance with the probability density $\rho(c_{ij})$. Crucial for this equivalence [15,17] is the fact that, at any finite time, the states σ_j of units j extending inputs to units i are uncorrelated for almost all i. Second, in constructing the update rule, it is helpful to note that that the Hamming distance D_t is the fraction of units i such that $\sigma_i^{(1)}(t) \neq \sigma_i^{(2)}(t)$.

In obtaining the specific form (3) used in our study, it has been assumed that all units have the same in-degree K. The K distinct units providing input to a given unit i are chosen randomly with equal probability from among the remaining

units $j \neq i$. For any such choice, the probability that s of the units i will have states that differ in the two replicas—i.e., $\sigma_i^{(1)}(t) \neq \sigma_i^{(2)}(t)$—*and* that the other $K-s$ units have coincident states at time t, is determined by simple combinatorics as

$$\binom{K}{s} D_t^s (1 - D_t)^{K-s}. \tag{A1}$$

More generally, the pattern of unit in-degrees will be expressed by a probability distribution. In Derrida's derivation, this is taken as a Poisson density, and a sum is performed over $K=1,\ldots,\infty$ with a weight factor $\bar{K}^K \exp(-\bar{K})/(K-1)!$.

Now consider the net input or "local field" $h_i(t)$ felt by generic unit i at time t, given by the quantity in square brackets in Eq. (1). The local fields corresponding to the two replicas are conveniently written as

$$h_i^{(1)}(t) = \sum_j c_{ij}\sigma_j^{(1)}(t) + h = u + v + h,$$

$$h_i^{(2)}(t) = \sum_j c_{ij}\sigma_j^{(2)}(t) + h = u - v + h. \tag{A2}$$

We observe that u and v are random variables, since they contain sums of random variables distributed according to the assumed probability density distribution $\rho(x)$ (with $x \in \{-\infty, +\infty\}$). For s running between 0 and K, denote by a_s the probability that the choices of these random variables will *not* lead to opposite signs of $\sigma_i^{(1)}(t+1)$ and $\sigma_i^{(2)}(t+1)$ for exactly s units i. Assembly of the equation of motion of the Hamming distance is completed by appending the probability factor a_s to the combinatoric factor (A1) and summing over s.

The first term on the right-hand side of Eq. (3) asserts unit probability that $\sigma_i^{(1)}(t+1)$ and $\sigma_i^{(2)}(t+1)$ have different signs for all N units i. The terms in the sum over s correct this overestimate for the specific events of stochastic updating within the annealed approximation carried out in the thermodynamic limit.

In the main text of this article, the coefficients a_s have been renamed as $I_s^{(K)}(\rho, h)$ to reflect the fact that in our analysis, the equation of motion for D_t is viewed from a somewhat different perspective than that described above. Rather than following the Hamming distance D_t between two replicas over some extended period, we focus on the effect on D_t over one time step, caused by any number s of spin flips $\sigma_i(t) \rightarrow -\sigma_i(t)$—as is required in an analysis of the stability of the fixed point $D_t = D^* = 0$ and thus for a determination of the critical boundary between ordered and chaotic behavior. We hasten to add that although Eqs. (3) and (4) with $a_s = I_s^{(K)}$ take account of all possible spin flips, the issue of stability is determined by the single integral $I_1^{(K)}$ through the condition (6) and the dynamical phase boundary through Eq. (11). We also note that at the fixed point $D^* = 0$, the leading term 1 on the right-hand side of Eq. (3) is canceled by the $s=0$ term, while all higher terms in the sum over s vanish as some power of D^*. [In fact, cancellation of the 1 term may be demonstrated straightforwardly for arbitrary D_t, through manipulation of the double sum in Eqs. (A3) and (A4) below.]

Since the late 1980s, distance-evolution equations resembling Eq. (3) have been employed to describe dynamical phases and associated critical conditions in a number of contexts. The fairly recent studies of Refs. [39,40] are typical, the first being concerned with canalizing Kauffman networks and the second with sociophysics models of opinion dynamics. In these studies, as well as in Derrida's original application to the dynamical phase transition from ordered to disorder behavior in spin glasses [16] and Kürten's early explorations [10,11] of the analogous phenomenon in neural-network models, the sum on the s index begins with $s=1$, rather than $s=0$ as in Eq. (3), and the leading term of unity appearing in Eq. (3) is absent. These differences stem from a contrary interpretation of the coefficient of the combinatoric factor (A1) as the probability that the choices made for the random variables u and v *will* lead to opposite signs for $\sigma_i^{(1)}(t+1)$ and $\sigma_i^{(2)}(t+1)$ for exactly s of the units i. The specific form of the equations adopted in Refs. [10,11], written in the notation of the present work, is

$$D_{t+1} = \sum_{k=1}^{K} (-1)^{k+1} \binom{K}{k} a_k D_t^k, \tag{A3}$$

with

$$a_k = 1 + \sum_{s=1}^{k} (-1)^s \binom{k}{s} I_s^{(K)}, \tag{A4}$$

where $I_s^{(K)}$ is the same integral as defined in Eq. (4).

Complementary and equivalent formulations can obviously be developed, in the annealed approximation, for the time evolution of the *overlap* $O_t = 1 - D_t$ of the states of two replicas.

[1] W. S. McCulloch and W. Pitts, Bull. Math. Biophys. **5**, 115 (1943).

[2] E. R. Caianiello, J. Theor. Biol. **2**, 204 (1961).

[3] J. J. Hopfield, Proc. Natl. Acad. Sci. U.S.A. **79**, 2554 (1982).

[4] S. A. Kauffman, J. Theor. Biol. **22**, 437 (1969).

[5] S. A. Kauffman, *Origins of Order: Self-Organization and Selection in Evolution* (Oxford University Press, Oxford, 1993).

[6] D. J. Watts and S. H. Strogatz, Nature (London) **393**, 440 (1998).

[7] A.-L. Barabási and R. Albert, Science **286**, 509 (1999).

[8] R. Albert and A. L. Barabási, Rev. Mod. Phys. **74**, 47 (2002).

[9] K. E. Kürten, in *Proceedings of the IEEE First Annual International Neural Network Conference, San Diego, 1987*, edited by Maureen Caudill and Charles Butler (IEEE, New York, 1987), Vol. II, p. 197.

[10] K. E. Kürten, in *Condensed Matter Theories*, edited by J. S.

Arponen, R. F. Bishop, and M. Manninen (Plenum, New York, 1988), Vol. 2.
[11] K. E. Kürten, Phys. Lett. A **129**, 157 (1988).
[12] K. E. Kürten, J. Phys. A **21**, L615 (1988).
[13] K. E. Kürten and H. Beer, J. Stat. Phys. **87**, 929 (1997).
[14] B. Derrida and Y. Pomeau, Europhys. Lett. **1**, 45 (1986).
[15] B. Derrida and G. Weisbuch, J. Phys. (Paris) **47**, 1297 (1986).
[16] B. Derrida, J. Phys. A **20**, L721 (1987).
[17] B. Derrida, E. Gardner, and A. Zippelius, Europhys. Lett. **4**, 167 (1987).
[18] J. W. Clark, J. Rafelski, and J. V. Winston, Phys. Rep. **123**, 215 (1985).
[19] J. W. Clark, K. E. Kürten, and J. Rafelski, in *Computer Simulation in Brain Science*, edited by R. M. J. Cotterill (Cambridge University Press, Cambridge, England, 1988), pp. 316–344.
[20] P. M. Binder and R. V. Jensen, Phys. Rev. A **34**, 4460 (1986).
[21] B. Luque and R. V. Solé, Phys. Rev. E **55**, 257 (1997).
[22] T. Rohlf and S. Bornholdt, Physica A **310**, 245 (2002).
[23] I. Nakamura, Eur. Phys. J. B **40**, 217 (2004).
[24] M. Aldana and P. Cluzel, Proc. Natl. Acad. Sci. U.S.A. **100**, 8710 (2003).
[25] P. R. Huttenlocher, Brain Res. **163**, 195 (1979); P. R. Huttenlocher, C. De Courten, L. J. Garey, and H. Van der Loos, Neurosci. Lett. **33**, 247 (1982).
[26] M. P. Stryker, J. Neurosci. **6**, 2117 (1986).
[27] A. W. Roe, S. L. Pallas, J. O. Hahm, and M. Sur, Science **250**, 818 (1990).
[28] M. F. Eckenhoff and P. Rakic, Dev. Brain Res. **64**, 129 (1991); J. P. Bourgeois and P. Rakic, J. Neurosci. **13**, 2801 (1993); J. Neurosci. Res. **102**, 227 (1994).
[29] J. Takacs and J. Hamori, J. Neurosci. Res. **38**, 515 (1994).
[30] G. M. Innocenti, Trends Neurosci. **18**, 397 (1995).
[31] J. R. Wolff, R. Laskawi, W. B. Spatz, and M. Missler, Behav. Brain Res. **66**, 13 (1995).
[32] E. Frank, Science **275**, 324 (1997).
[33] D. Purves and J. W. Lichtman, Science **210**, 153 (1980); J. W. Lichtman, Semin. Dev. Biol. **6**, 195 (1995).
[34] M. J. Barber and J. W. Lichtman, J. Neurosci. **19**, 9975 (1999).
[35] E. Henneman, J. Exp. Biol. **115**, 105 (1985).
[36] H. Sompolinsky, Phys. Rev. A **34**, 2571 (1986).
[37] G. Chechik, I. Meilijson, and E. Ruppin, Neural Comput. **10**, 1759 (1998).
[38] K. Mimura, T. Kimoto, and M. Okada, Phys. Rev. E **68**, 031910 (2003).
[39] A. A. Moreira and Luis A. Nunes Amaral, Phys. Rev. Lett. **94**, 218702 (2005).
[40] S. Galam, Europhys. Lett. **70**, 705 (2005).